Cell Reports

Article

Transient sensorimotor projections in the developmental song learning period

Graphical abstract

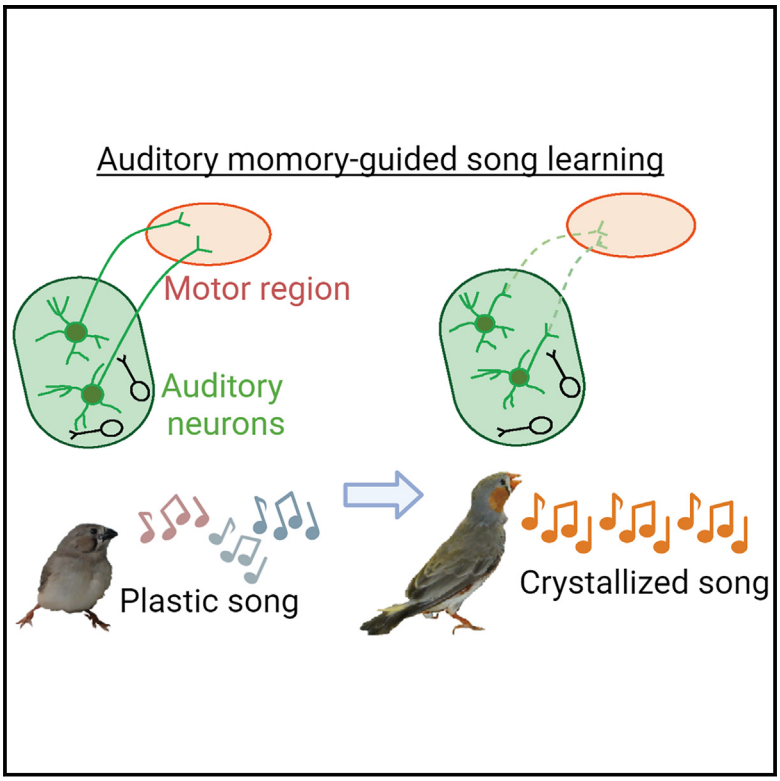

Authors

Matthew I.M. Louder, Masafumi Kuroda, Daisuke Taniguchi, ..., Yasushi Okada, Hiroyuki Hioki, Yoko Yazaki-Sugiyama

Correspondence

yazaki-sugiyama@oist.jp

In brief

Auditory memory guidance for motor shaping is necessary for vocal learning. Here, Louder et al. show transient axonal projections to the song premotor area from the neurons responsive to the tutor's song (TS) playback in the auditory forebrain. Ablating TS-responsive neurons disrupts song learning in juveniles but not in adults.

Highlights

- Specific manipulation of song-responsive neurons with a cFos-TetON system is created
- Ablating tutor's song (TS)-responsive neurons prevents juveniles from song learning
- TS-responsive neurons transiently project to song premotor area, HVC, in juveniles
- Sensory isolation does not delay song crystallization or axon pruning in HVC

Louder et al., 2024, Cell Reports *43*, 114196
May 28, 2024
https://doi.org/10.1016/j.celrep.2024.114196

CellPress

Cell Reports

CellPress
OPEN ACCESS

Article

Transient sensorimotor projections in the developmental song learning period

Matthew I.M. Louder,[1,9] Masafumi Kuroda,[1,2,9] Daisuke Taniguchi,[1,2] Joanna Agnieszka Komorowska-Müller,[3] Yuichi Morohashi,[3] Megumu Takahashi,[4,5] Miguel Sánchez-Valpuesta,[6] Kazuhiro Wada,[6,7] Yasushi Okada,[1,2,8] Hiroyuki Hioki,[4] and Yoko Yazaki-Sugiyama[1,3,10,*]

[1]International Research Center for Neurointelligence (WPI-IRCN), The University of Tokyo, Bunkyo-ku, Tokyo 113-0033, Japan
[2]RIKEN Center for Biosystems Dynamics Research (BDR), Suita, Osaka 565-0874, Japan
[3]Neuronal Mechanism of Critical Period Unit, OIST Graduate University, Kunigami, Okinawa 904-0495, Japan
[4]Department of Neuroanatomy, Juntendo University Graduate School of Medicine, Bunkyo-ku, Tokyo 113-8421, Japan
[5]Center for Genomic and Regenerative Medicine, Juntendo University Graduate School of Medicine, Bunkyo-ku, Tokyo 113-8421, Japan
[6]Graduate School of Life Science, Hokkaido University, Sapporo, Hokkaido 060-0810, Japan
[7]Faculty of Science, Hokkaido University, Sapporo, Hokkaido 060-0810, Japan
[8]Department of Cell Biology, Department of Physics, and Universal Biology Institute (UBI), The University of Tokyo, Bunkyo-ku, Tokyo 113-0033, Japan
[9]These authors contributed equally
[10]Lead contact
*Correspondence: yazaki-sugiyama@oist.jp
https://doi.org/10.1016/j.celrep.2024.114196

SUMMARY

Memory recall and guidance are essential for motor skill acquisition. Like humans learning to speak, male zebra finches learn to sing by first memorizing and then matching their vocalization to the tutor's song (TS) during specific developmental periods. Yet, the neuroanatomical substrate supporting auditory-memory-guided sensorimotor learning has remained elusive. Here, using a whole-brain connectome analysis with activity-dependent viral expression, we identified a transient projection into the motor region, HVC, from neuronal ensembles responding to TS in the auditory forebrain, the caudomedial nidopallium (NCM), in juveniles. Virally induced cell death of the juvenile, but not adult, TS-responsive NCM neurons impaired song learning. Moreover, isolation, which delays closure of the sensory, but not the motor, learning period, did not affect the decrease of projections into the HVC from the NCM TS-responsive neurons after the song learning period. Taken together, our results suggest that dynamic axonal pruning may regulate timely auditory-memory-guided vocal learning during development.

INTRODUCTION

Acquiring motor skills to suit our environment during development, such as learning a local dialect, is crucial for survival in social contexts. Well-organized sensory-motor coordination is necessary to develop proper higher cognitive functions, such as language skills, through experience.[1] Like human speech development, songbirds learn to sing acoustically complex motor patterns—songs—by repeatedly hearing and vocally mimicking a tutor singing during the developmental critical period. Young zebra finches, a premier model of songbirds, listen and memorize their tutor's songs (TSs; normally their father's song) during the initial auditory phase and then gradually align their own vocalizations to the memorized template while shaping a uniquely individual adult crystalized song during a sequentially overlapping sensorimotor phase. Singing a stable stereotyped song is necessary for attracting females to establish pair bonding and for preserving identity.

Male zebra finches crystallize a song motor pattern at a certain time during development, even with immature abnormal acoustic structure under socially isolated conditions.[2–4] The amount of learning from a TS varies depending on the individual, suggesting that the timing of stabilizing song is not based on similarity to a TS. How these auditory memories guide motor learning to mimic a TS while acquiring variations in vocal pattern for individual uniqueness before crystallizing a final song in due time has remained elusive.

Several studies suggest that the TS memory acquired in the auditory phase is stored in the caudomedial nidopallium (NCM),[5,6] analogous to the mammalian higher auditory cortex. Recently, we reported that a subset of NCM neurons exhibit highly selective auditory responses to the playback of a TS within some days after tutoring experiences, suggesting the creation of TS memory neuronal ensembles.[7,8] Yet, classic neuronal tract-tracing studies in adults failed to find direct axonal connections from the NCM into the HVC (used as a proper name), a premotor locus required for song patterning.[9] Here, we established an innovative, brain-wide connectome approach in zebra finches from functionally targeted neurons to identify the anatomical substrate for auditory-memory-guided vocal motor acquisition.

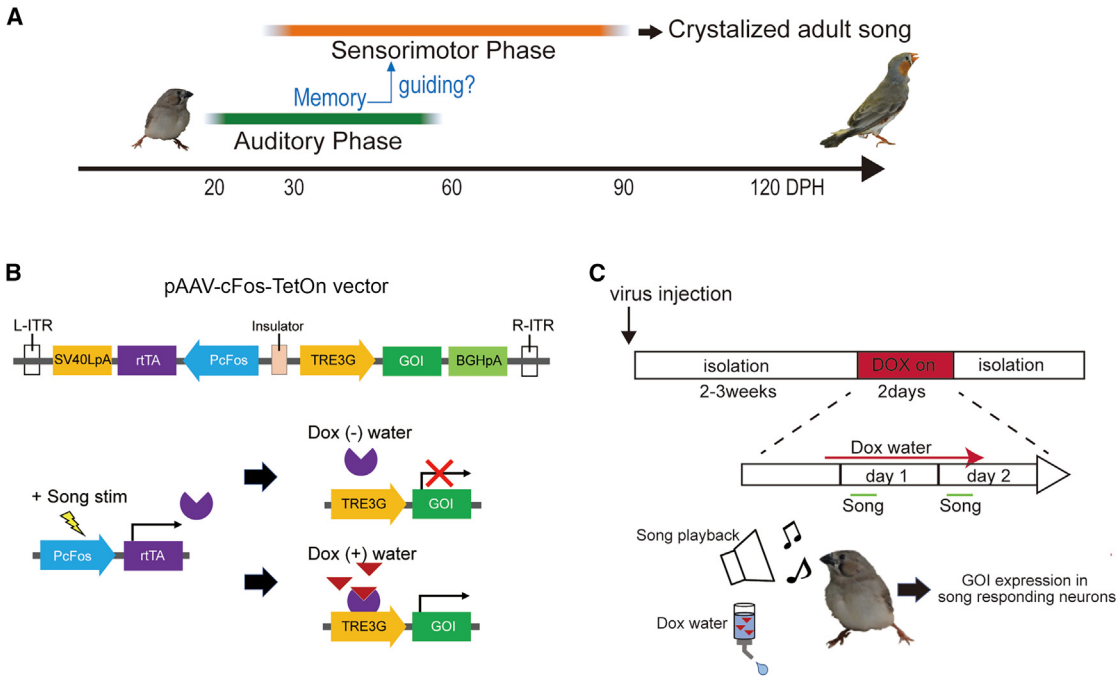

Figure 1. Designs of AAVs for expressing GOIs in TS-responsive neuronal ensembles

(A) The timeline of zebra finch's critical song learning period during development. During the sensory phase, a juvenile listens to a tutor and forms a memory of that song. During the sensorimotor phase, the bird matches its own vocalizations to the memorized song through auditory feedback. The song becomes stable and crystalizes around 90 days post-hatching (DPH).

(B) Adeno-associated viral (AAV) vector employing cFos-TetON system to express genes of interest (GOIs). The reverse tetracycline transactivator (rtTA) and TRE3G promotor are separated by the insulator, and the translated rtTA protein can bind to the TRE3G promoter only in the presence of doxycycline (DOX).

(C) Experimental timeline for EYFP expression in song-responsive neurons *in vivo* with cFos-TetON system. Two to three weeks after virus injection, birds were provided with DOX water starting the night before song playback, which was provided in the next 2 days (ended just after song playback on the second day). Birds were sacrificed 4 days after the second day of song playback.

This technique revealed a transient projection from TS-responsive neurons in the NCM into the HVC during the developmental song learning period. Targeted viral lesions of this selected population of neurons during the song learning period, but not in adulthood, prevented juveniles from learning a TS. Taken together, our results suggest that a transient NCM-HVC memory projection may regulate timely song learning during development.

RESULTS

TS-responsive NCM neuronal ensembles guide song motor learning

Juvenile zebra finches learn to sing from early auditory experiences with their tutor (Figure 1A). We previously reported that a small subset of neurons (~15% of broader-spiking neurons) within the NCM, a relatively large structure with no clear boundaries, become highly selective to TS playback after listening to their tutor singing.[7,8] This suggests that a subpopulation of neurons in the NCM form a memory of the TS during the auditory phase of song learning. To visualize and investigate the function of these NCM neurons, we implemented techniques to directly access TS-responsive neurons during precise periods of song learning. Methods established in rodents have utilized adeno-associated viral (AAV) vectors expressing genes of interest (GOIs) under the control of an immediate-early gene promotor and doxycycline (DOX)[10–12] (Figure 1B). These techniques could allow the direct manipulation of TS-responsive neurons and avoid non-specific manipulation of a large number of neurons that might not be directly related to tutor song memories.

First, we tested if AAVs with a cFos promotor and tetracycline (TetON) system express GOIs specifically in those NCM neurons activated by hearing the TS (Figure 1C). We constructed an AAV, which induces EYFP expression only in activated neurons in the presence of DOX (AAV-cFos-TetON-EYFP-PEST). Zebra finch adults injected with the AAV-cFos-TetON-EYFP-PEST in the NCM were exposed to TS playback concurrent with DOX in their drinking water to induce EYFP expression only in TS-responsive neurons (Figure 1C). Control birds that only received DOX with no song playback displayed fluorescence in fewer neurons (Figures S1B and S1C), indicating that EYFP-expressing neurons in experimental birds could be considered responsive to TS playback.

To determine if these TS-responsive NCM neuronal ensembles contributed to song learning, we selectively ablated them with other AAVs that induce cell death in TS-responsive neurons by expressing constitutively active caspase-3 (CaCasp3) or diphtheria toxin A (dtA) (AAV-cFos-TetON-CaCasp3 and AAV-cFos-TetON-dtA, respectively) (Figure 2A).[13] Juveniles were raised with their tutor and injected with ablating AAVs in the

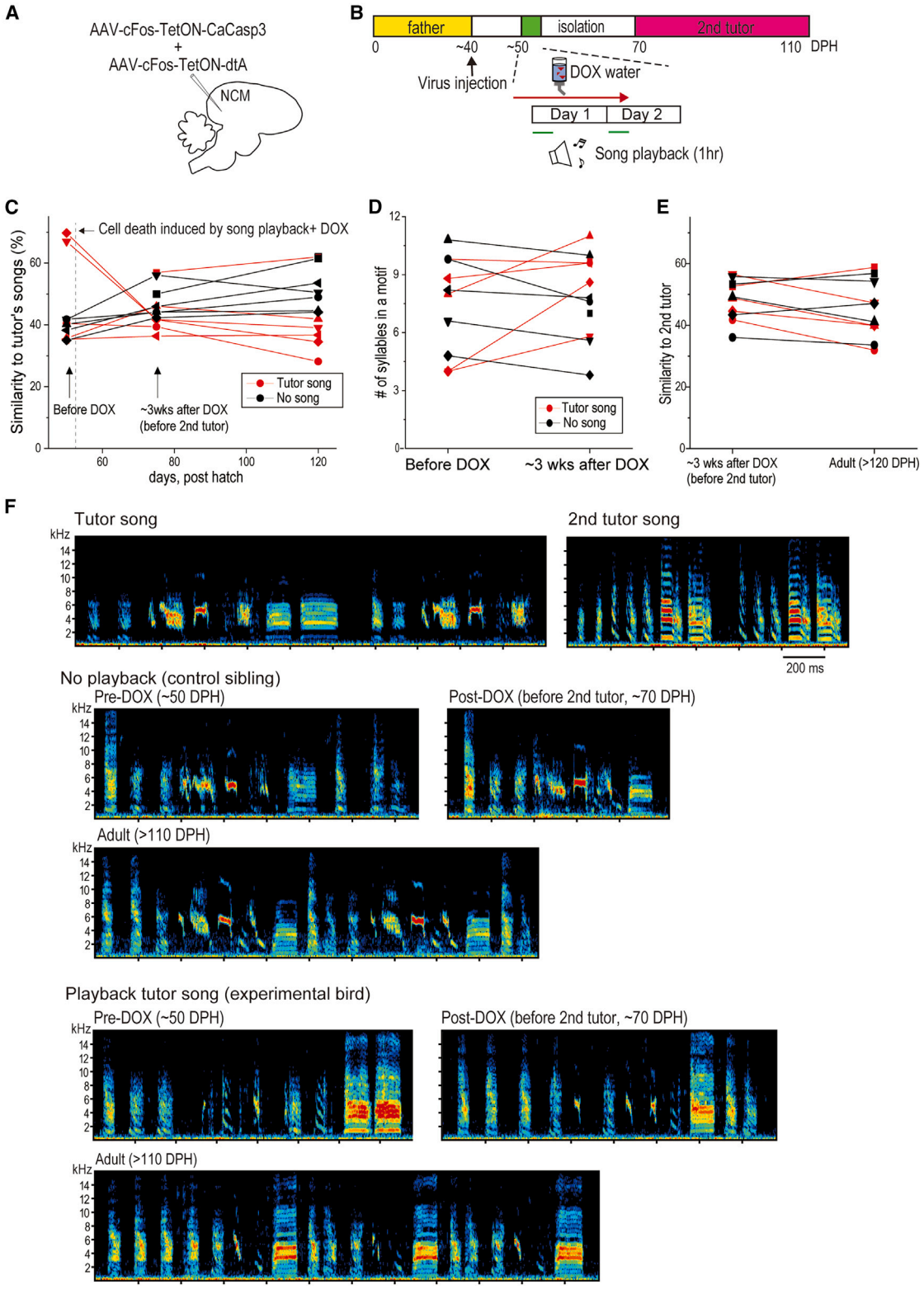

(legend on next page)

NCM at ~40 days post-hatching (DPH) and subsequently isolated. Birds were provided with DOX water and exposed to TS playback at 50–55 DPH to induce cell death in neurons activated by TS playback (Figure 2B). Controls were siblings raised together undergoing the same experimental procedures, including DOX, but were not exposed to song playback. To test learning, song similarity to the TS was tracked over development (Figures 2C and 2F).

The song similarities to TSs between groups exposed to TS and no song were not significantly different at any time points (50, 75, and 120 DPH, $p > 0.05$, one-way repeated measure ANOVA with post hoc Fisher's LSD test). However, by directly comparing the songs of experimental and control siblings, which were exposed to the same amount of singing from the same tutor, we found that songs of birds in which TS-responsive neurons were ablated were significantly less similar to the TSs in adults (>120 DPH) than those of the control siblings (Figure 2C, at 120 DPH, $p = 0.028$, paired t test, df = 5, $N = 6$ and 6). While two birds displayed the highest song similarity to the TS at 50 DPH, prior to treatment, their similarity decreased after TS-responsive neuron ablation with DOX water and TS playback and persisted into adulthood (Figures 2C and S2).

As zebra finch songs develop, they become rhythmic, and syllable sequences become less variable, as reflected in a shorter motif size. In contrast, isolated birds that are not exposed to a tutor sing arrhythmic songs with variable syllable sequences and much longer motifs.[14–16] To see if TS-responsive neurons contribute to such song sharpening, we compared motif size before and after TS-responsive neuron ablation. All control birds (5/5) decreased the number of syllables in a song motif (before vs. after TS-responsive neuron ablation; $p = 0.023$, paired t test). Instead, most birds (4/5) with TS-responsive neuron ablation at ~50 DPH rather tended to increase motif length by adding novel syllables by ~70 DPH, 3 weeks after the induction of cell death, and the number of syllables in a motif was not different before and after TS-responsive neuron ablation ($p = 0.076$, paired t test) (Figure 2D). Taken together, these results suggest that juveniles with TS-responsive neuron ablation in the NCM did not lose their motor ability to change their vocalizations but failed to refine their songs to match the TS.

The absence of a tutor can extend the auditory phase of learning, as no auditory memory is created, and juvenile learning remains plastic.[2–4] We tested if inducing cell death in TS-responsive neurons would itself re-open the auditory learning period, comparable to no memory formation by social isolation throughout this phase. We exposed juveniles to a second tutor by housing both experimental and control siblings with a novel zebra finch (2nd tutor) starting at 70 DPH, 3 weeks after the induction of cell death. Neither the experimental nor control birds learned from the second tutor (Figure 2E), suggesting that ablating TS-responsive neurons did not re-open the sensory phase. Delayed cell death at the end of the song learning period (90 DPH) also did not disrupt learning and singing (Figure S3A): there was no difference before and after TS-responsive neuron ablation in the similarity between the TS and birds' own song (Figure S3B) or between experimental and control birds in the similarity of their songs before and after ablation (Figure S3C). Overall, these experiments suggest that TS-responsive neuronal ensembles in the NCM enable vocal motor learning from auditory templates but do not underlie extending the auditory phase when lost.

Visualizing brain-wide TS auditory memory neuronal ensembles in the zebra finch brain

To visualize the sparse network of TS-responsive neurons in the NCM and their axonal projections, we imaged the whole brain using tissue-clearing methods (X-CLARITY and Logos DeepLabel Antibody Staining). EYFP signals were enhanced and examined with a custom-made light-sheet fluorescence microscope (LSFM), which can accommodate an entire brain area without tiling in the x-y plane for each z-position within one visual field. We then established an axonal registration system for our LSFM images at each z-position to trace the axonal projections (Figures S4A and S4B).

We registered axonal projections onto 3D zebra finch brain maps, which we assembled from nuclear staining with propidium iodide. We found axons of TS-responsive NCM neurons in two adults projecting into only four brain sites across the whole brain (Figures S5A and S5B), all of which correspond to song listening or singing: (1) two auditory areas, the caudomedial mesopallium (CMM) and HVC-shelf, reported to project onward to the HVC.[9,17,18] Most of the ventro-lateral axonal trajectories terminated in the HVC-shelf but projected rarely to only the posterior part of the HVC (Figure S5B; Videos S1 and S2). (2) The ventral portion of the intermediate arcopallium (AIV), where neurons receive input from auditory cortical areas, such as Field L, the CMM, and HVC-shelf, perhaps as auditory feedback signals

Figure 2. Ablating NCM TS-responsive neurons prevents juveniles from copying a TS

(A and B) Virus constructs and experimental timeline of cell death induction in the neurons that were activated by TS playback.

(C) Song similarity of the bird's own songs to the TSs at each developmental time point in which cell death was induced by DOX administration with exposure either to TS or no song playback. Song similarity to TS in the birds exposed to TS to induce cell death was significantly smaller than those in the control siblings, which were provided with DOX and no songs ($p = 0.028$, paired t test, df = 5, $N = 6$ and 6) at 120 DPH, but was not different at 75 DPH ($p = 0.33$, paired t test, df = 5, $N = 6$ and 6) (the same symbols denote siblings).

(D) The number of syllables in a motif of the song in birds exposed to TS and no song before and ~3 weeks after cell death induction (DOX application). The number of syllables in a motif was significantly different between before and after TS-responsive neuron ablation in control sibling birds ($p = 0.023$, paired t test, df = 4, $N = 5$) but not in the birds that were TS-responsive neuron ablated ($p = 0.076$, paired t test, df = 4, $N = 5$).

(E) Song similarity to the second tutor in the birds exposed to TS and no song at ~3 weeks after cell death induction (DOX application) and as adults (>120 DPH).

(F) Representative sound spectrograms of TS, second TS, and songs of the bird exposed to no song (control sibling) (top) and the experimental bird exposed TS (bottom) during DOX application at before cell death induction (pre-DOX, ~50 DPH), ~3 weeks after DOX application (post-DOX, before 2nd tutor, ~70 DPH), and in adults (>110 DPH).

See also Figures S2 and S3.

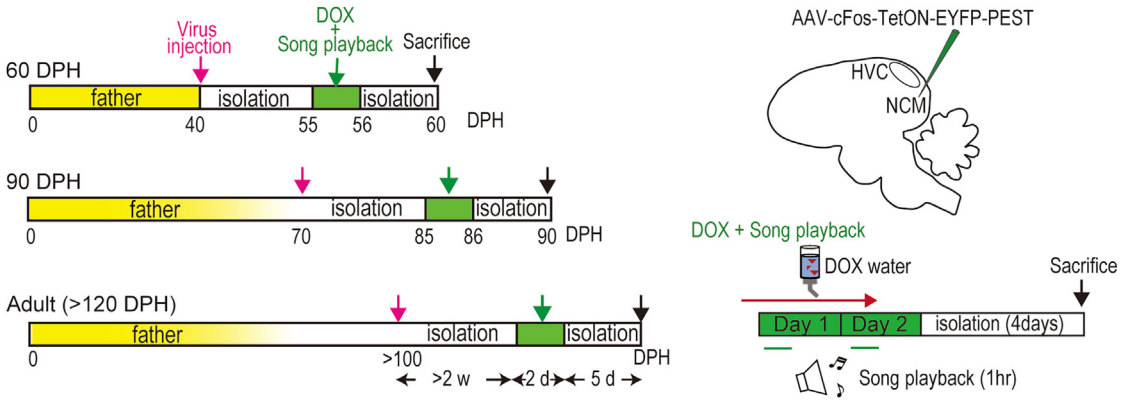

Figure 3. Experimental design for visualizing TS-responsive neurons in the NCM at various ages

Experimental timelines for each experimental age group of birds. All birds were provided with DOX and TS playback for 2 days and then sacrificed 4 days later.

during singing.[18–20] Finally, (3) long-distance axonal tracts terminating in Area X, the basal ganglia locus in the "song system" was observed, but which curiously passed through the neighboring latera magnocellular nucleus of the anterior neostriatum (LMAN) (Figure S5B; Videos S1 and S2).

Developmental disconnection of TS-responsive neuronal projections in motor control regions

Whole-brain axonal tracing from TS-responsive cell bodies in the NCM showed projections into the song system. We then further quantified axonal projections into the premotor region, the HVC, over the developmental song learning period with conventional histological brain sections. Zebra finches were injected with the AAV-cFos-TetON-EYFP-PEST at various ages and exposed to TS playback 2–3 weeks after virus injection with DOX provided in the drinking water (Figure 3). The number of EYFP-expressing neurons in the NCM varied across birds of all ages, as it is impossible to precisely control the amount of virus expression (Figures 4A and 4B).

Strikingly, further quantification of axonal projections revealed a transient NCM projection into the HVC over the song development period (Figures 5A and 5B). There was a dense projection from TS-responsive NCM neurons into the juvenile HVC during the sensorimotor phase of song learning (60 DPH), with a trend for more projections into the HVC in the right hemisphere (Figure S6A). In contrast, older juveniles near the end of the sensorimotor phase (90 DPH) and adults (>120 DPH) displayed the most TS-responsive axons within the HVC-shelf, and not in the HVC, as indicated by a significantly lower ratio of anti-GFP-positive area between the HVC and HVC-shelf ($p < 0.05$, ANOVA with post hoc Tuckey LSD test, Figure 5B). These results suggest a disconnection of NCM-HVC projections by the end of the sensory phase of song development.

Notably, we found fewer EYFP-expressing neurons in the NCM and fewer projections within the HVC in 60 DPH juveniles stimulated with a novel zebra finch song (conspecific song; lower ratio of anti-GFP-positive area and smaller proportion of anti-GFP-positive area within the HVC, with both not significantly different from 60 DPH juveniles exposed to TS) (Figures 4B, 4C, and S6A–S6C). This suggests that projections to the HVC were from TS-responsive neurons in the NCM. The lower ratio of anti-GFP-positive area between the HVC and HVC-shelf was also found in birds injected with AAV-cFos-TetON-EGFP (note: no PEST sequence included to prevent signal decay) at ~40 DPH and provided with DOX water and TS playback to induce EGFP expression in TS-responsive NCM neurons at ~55 DPH and then sacrificed at ~90 DPH (Figures 4B and 5B, 90 DPH, open symbols, and S6D).

The lower ratio of anti-GFP-positive area between the HVC and HVC-shelf was also confirmed by significantly greater proportions of the anti-GFP-positive area within the HVC in 60 DPH juveniles than in 90 DPH juveniles, while proportions of the anti-GFP-positive area within the HVC-shelf were no different between 60 and 90 DPH juveniles and adults (Figure S7A). The number of NCM neurons that expressed EYFP varied across birds, but the proportion of anti-GFP-positive area normalized by the number of EYFP-expressing neurons in the NCM in 60 DPH juveniles was greater than, yet not significantly different from, that of 90 DPH juveniles and adults (Figure S7B). Combined with prior failures to detect direct anatomical input from the adult NCM to the HVC using classical tracer injections,[9] the lower ratio of anti-GFP-positive area between the HVC and HVC-shelf in adults was considered to be due to fewer projections from NCM neurons rather than low or off-target viral expression. Taken together, these results suggest that a transient axonal projection from TS-responsive NCM neurons into the HVC is pruned during development, instead of a progressive decline in NCM auditory response to TS (and fewer GFP expressions).

To confirm and further establish a detailed time course of the transient NCM-HVC projection in juveniles, we examined axonal projections in different subsets of juveniles between 70 and 90 DPH. The density of projections into the HVC in 70 DPH juveniles was significantly higher than that of 80 and 90 DPH juveniles, as indicated by the lower ratio of anti-GFP-positive area between the HVC and HVC-shelf ($p < 0.05$, ANOVA with post hoc Tuckey LSD test, Figures 6A and 6B). To probe the transient TS-responsive projection with respect to song crystallization, we measured similarities between the songs on the day of sacrifice for histological observation and the songs 10 days prior. Indeed, there was a significant negative correlation between the density of

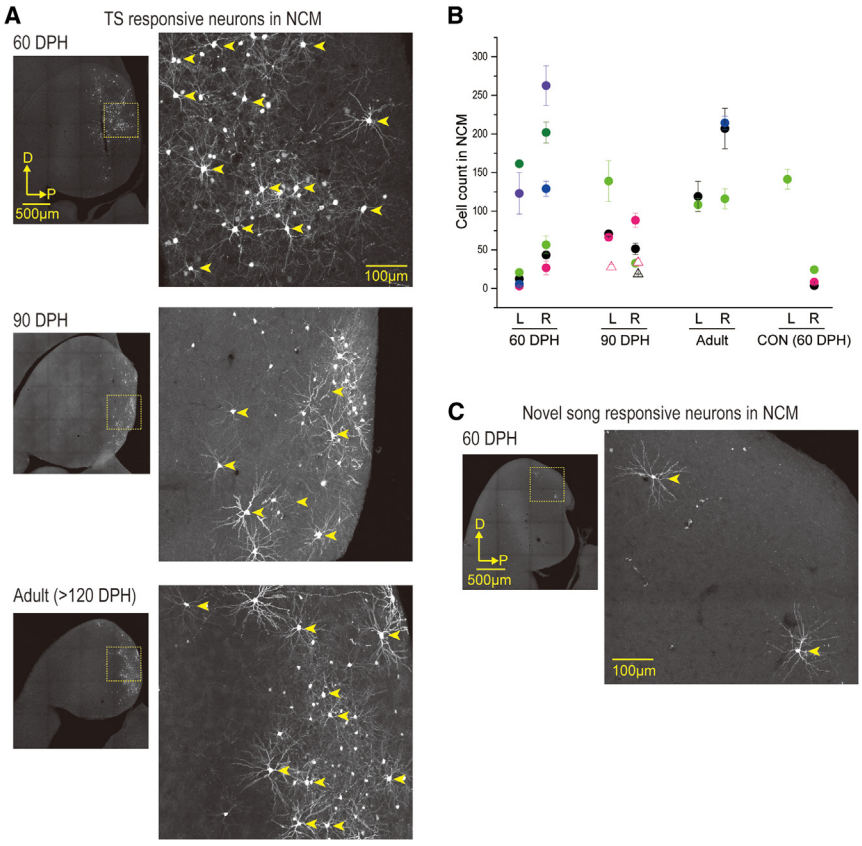

Figure 4. TS-responsive neurons in the NCM

(A) Representative confocal images of virus injection sites in the NCM (left) and a magnified view of the rectangular area (right) of the bird, which was injected with the AAV-cFos-TetON-EYFP-PEST and received TS playback under DOX administration at 60 and 90 DPH and as adults (>120 DPH). The yellow arrowheads point to representative TS-responsive neurons. Scale bars: 500 μm (left) and 100 μm (right).

(B) The average number of neurons that expressed EYFP in a section (mean and SEM over three sections) in the birds that underwent the experiments described in Figure 3 at 60 and 90 DPH and as adults (>120 DPH) and the birds that underwent the same experiment at 60 DPH but were exposed to novel zebra finch song (conspecific song [CON]) playbacks. The same symbol and color denote the data from the same birds in Figure S6A.

(C) Representative confocal images of neurons in which EYFP expressions were induced by playback of a novel zebra finch song with DOX administration. Novel song playback induced EYFP expression in a few neurons, indicated with yellow arrowheads. Scale bars: 500 μm (left) and 100 μm (right).

axonal projections within the HVC, measured as the ratio of anti-GFP-positive area in the HVC vs. HVC-shelf, and the similarity between birds' own songs on the day of sacrifice and 10 days prior ($r = -0.85$, $p < 0.05$, Figures 6C and 6D). This suggests that the transient projection from TS-responsive NCM neurons into the HVC is involved in song crystallization. In contrast, there was no correlation between NCM projection density into the HVC and the similarity of birds' own song to the TS (linear regression, $r^2 = 0.31$, $r = -0.56$, $p > 0.05$).

Experience dependency for disconnecting NCM-HVC axonal projections

We found a transient projection into the HVC from NCM TS-responsive neuronal ensembles, which was necessary for song learning. To see if the NCM-HVC projections and pruning were dependent upon song learning, we tested whether exposure to the tutor itself, known to affect the timing and strength of song learning, impacts the time course of NCM-HVC projection dynamics. As auditory isolation from TS delays closure of the sensory learning period,[2–4] we examined the connections between TS-responsive NCM neurons and the HVC in the absence of tutoring.

Juveniles were isolated from their father and raised by their mother and siblings starting at 10–12 DPH in a sound attenuation chamber, which prevented them from learning a TS. Birds were injected with AAV-cFos-TetON-EYFP-PEST into the NCM at 70–75 DPH. They were then housed alone until they rejoined their siblings (when available) and a tutor for 7–13 days before receiving DOX water and TS playback for 2 days at ~90 DPH (Figure 7A). These birds failed to copy the TS they were exposed to starting at ~75 DPH and had crystallized songs like juveniles that were isolated at a similar age.[4]

These birds displayed EYFP expression in a subset of NCM neurons, as observed in normally reared age-matched birds (90 DPH) (Figures 7B and 7C). Axons were found in the CMM and dorso-lateral to the HVC but were not seen within the HVC proper, as indicated by the low ratio of anti-GFP-positive area between the HVC and HVC-shelf (Figures 7B and 7C). Taken together, these results suggest that song memory ensembles in the NCM, formed beyond the typical song learning period, neither induce sensorimotor learning[4] nor project into the HVC. However, the possibility cannot be excluded that NCM-HVC projections formed with delayed song memory formation with tutoring at ~75 DPH retracted quickly without any timing delay with isolation by ~90 DPH.

DISCUSSION

Zebra finches are highly social, using vocal communication both in males and females to mediate a variety of cognitive behaviors, such as developmental song learning, mate choice, and territorial identification among others. Here, we established methods for labeling functionally distinct neuronal subsets and tracing their brain-wide axonal projections in the songbird brain. This revealed a transient, developmental projection from TS-responsive neurons in the auditory cortical area, the NCM, directly into the motor area, the HVC.

The NCM is thought to be involved in various cognitive functions. Lesion or inactivation of the NCM disrupts pitch

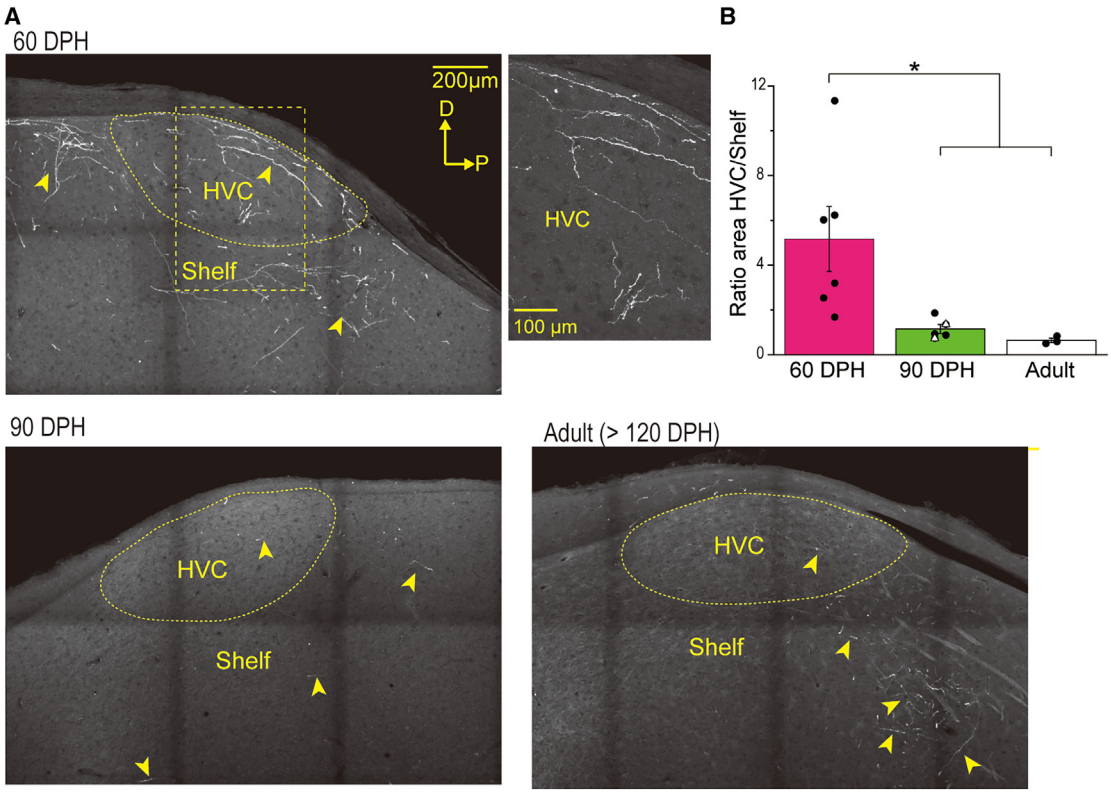

Figure 5. Transient neuronal projections from NCM TS-responsive neurons into the HVC during the song learning period

(A) Representative confocal images of HVC in the birds described in the experiment in Figure 3 at 60 and 90 DPH and as adults (>120 DPH) (scale bar: 200 μm) and enlarged image of HVC area indicated as square in the 60 DPH box (top right, scale bar: 100 μm). Sections are from the same bird and hemisphere as in the sections in Figure 4A.

(B) Averaged (mean and SEM) ratio of the area detected as positively stained with GFP antibody between HVC and HVC-shelf in birds that underwent the experiment described in Figure 3 at 60 and 90 DPH and as adults (>120 DPH). Each dot denotes an individual bird (average of three sections from each hemisphere). Open triangles in the 90 DPH box are from the birds that were administered DOX and TS playback at 55 DPH and sacrificed at 90 DPH. The ratio of the birds at 60 DPH is significantly different from the birds at 90 DPH and adults ($p < 0.05$, ANOVA with post hoc Fisher's LSD test, $N = 6$, 5, and 3 for the birds at sacrificed at 60, 90, and >120 DPH, respectively).

See also Figures S6 and S7.

discrimination after training in adult male zebra finches[21] and decreases song preference in adult females.[22] We recently found that a small subset (~15%) of neurons in juveniles show highly selective auditory responsiveness to a learned TS,[7,8] in contrast to other brain loci in the song system where nearly all neurons are selective to the bird's own song.[23–25] Here, we identified neuronal ensembles responsive to the TS that send axonal projections directly into the HVC only in juveniles.

Zebra finches learn to sing by first memorizing a TS and then matching their vocal output to that memory via auditory feedback. They develop their songs similarly, but not identically, to the TS. It is thought that a song motor template is formed. Studies in adult zebra finches have found that reinforcement learning can shift the fundamental frequency of targeted syllables, but once released from reinforcement, the birds revert to the original fundamental frequency, suggesting that the motor template is preserved after initial song learning.[26,27] TS memory might be different from song motor templates and might not be used once birds establish their own song. Our previous study in juveniles revealed a subset of neurons in the NCM that respond exclusively to the TS and not to their own songs after song learning, suggesting that these neurons may be a neuronal substrate of TS auditory memory.[7,8] These neuronal ensembles are presumably the major target of AAVs used in this study, as they should strongly respond to the TS. Further studies are needed to identify the kind of information carried by their transient NCM-HVC projection.

"Developmental exuberance"—the overproduction of axonal projections—of both macroscopic ones between two or more brain regions and microscopic, local cortical ones is well known in mammalian brain networks (reviewed in Innocenti and Price[28]). Overlapping axons are eliminated or remodeled by selection during the development of refined tuning (e.g., visual ocular dominance columns, cerebellar climbing fibers, motor axons). Transient embryonic connections also guide later development of axonal projections.[29] In zebra finches, axonal projections from HVC to the motor region, robust nucleus of the arcopallium (RA) start to increase when juvenile birds start to sing (~30 DPH), and synaptic connections decrease in number while increasing in strength during song maturation.[30] In contrast,

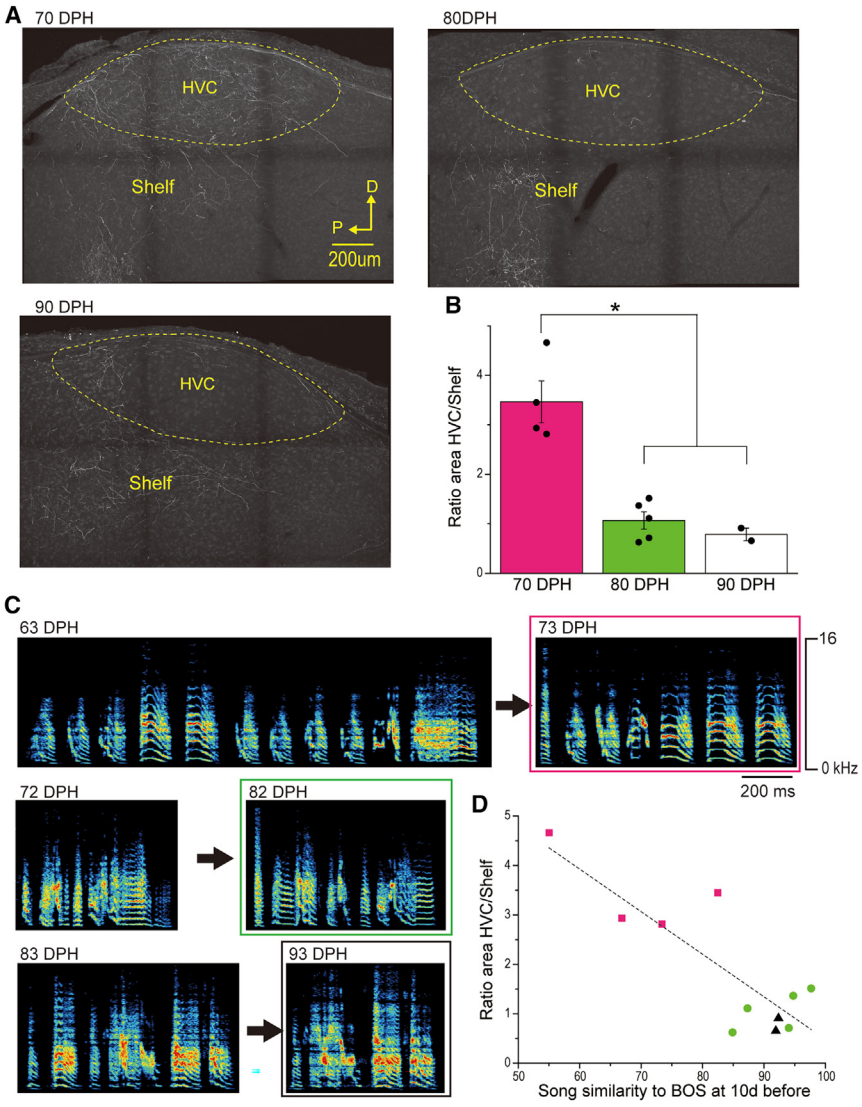

Figure 6. Neuronal projections from NCM TS-responsive neurons into the HVC correlate with developmental song changes

(A) Representative confocal images of HVC in the birds that underwent the experiment described in Figure 3 but injection with AAV at ~50, 60, and 70 DPH and sacrificed at ~70, 80, and 90 DPH, respectively. Scale bar: 200 μm.

(B) Average ratio of the area (mean and SEM) detected as positively stained with GFP antibody between HVC and HVC-shelf in the birds described in Figure 3 but injected with virus at ~50, 60, and 70 DPH and sacrificed at ~70, 80, and 90 DPH, respectively. Each dot denotes the data of individual birds (average of three sections from each hemisphere). The ratio of the 70 DPH birds is significantly different from that of the 80 and 90 DPH birds ($p < 0.05$, ANOVA with post hoc Fisher's LSD test).

(C) Representative sound spectrograms of songs on the day birds were sacrificed (73, 82, or 93 DPH) (right) and 10 days before the sacrifice day (left).

(D) Plots of the song similarity between songs at the sacrifice day and 10 days before against the ratio of the area detected as positively stained with the GFP antibody between HVC and HVC-shelf in the same birds. There is a significantly negative correlation (linear regression, $r^2 = 0.71$, $r = -0.85$, $p < 0.05$).

connections from the LMAN to the RA are established earlier (~20 DPH) and refined into topographical projections later in development (reviewed by Bottjer[31]). Lesions of the LMAN alter the input from the HVC to the RA.[32] In this study, we found that NCM-HVC disconnection seems to occur at an even later stage of development (70–80 DPH). This might shape the time window of song motor learning, as we found a negative correlation between NCM projection density into the HVC and the level of song crystallization.

Notably, our findings reveal the long-sought interareal projection from a functionally distinct neuronal ensemble in an auditory region to a motor region that is dynamic and transient during the critical developmental song learning period. Ablations of this specific neuron ensemble during song learning, but not later, prevented juveniles from learning their TS. Concomitant with the lack of song learning under social isolation, projections from this NCM neuronal ensemble were not observed in the motor region. This transient interareal developmental exuberance might balance the expanding possibilities of acquiring new song elements while ensuring consistent motor patterns by limiting the temporal window for sensory-guided motor learning. Developing and maintaining unique stereotyped songs are vital strategies for mating success and territorial identification, while adopting culture-specific dialects is essential for social harmony.

Strikingly, sensory isolation, which delays the closure of the sensory learning period, did not delay the decrease of NCM-HVC projections. While isolation causes birds to develop abnormal songs, they crystallize their songs within a normal song learning period, suggesting a programmed timing of song acquisition. Several experiments, such as manipulating the timing of NCM-HVC axonal projections/pruning or testing if seasonal song learners retain sensorimotor connections in adulthood, await further investigation to both reveal the underlying neuronal mechanism regulating the timing of developmental song learning period and answer how they balance enhanced perceptual capacities with establishing stable motor patterns.

Limitations of the study

Here, we established techniques for labeling and ablating functionally distinct neuronal ensembles by implementing the cFos-TetON system using a virus injection into a region of interest in the songbird brain. Using this technique, we found transient neuronal projections from TS-responsive neurons in the auditory

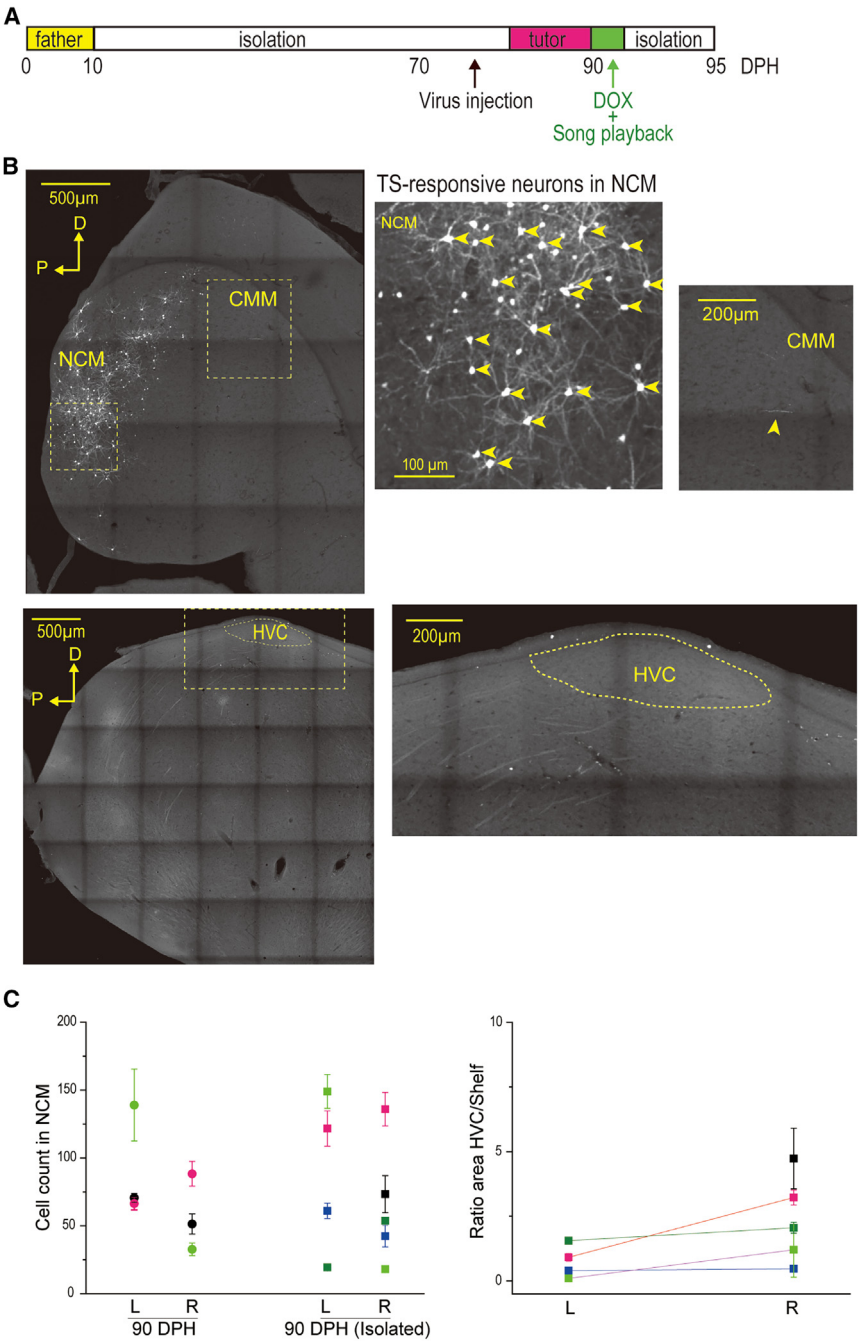

Figure 7. Anatomical characters of TS-responsive neurons in isolated birds

(A) Experimental design for isolation. Birds were isolated starting at 10–12 DPH and housed with a tutor for 7–13 days starting at 70–75 DPH after the AAV vector injection (AAV-cFos-TetON-EYFP). They were then exposed to TS playback together with DOX water administration for 2 days at 90 DPH and were sacrificed at 95 DPH.

(B) Representative confocal images of the virus injection site in the NCM (top left, scale bar: 500 μm). Representative TS-responsive neurons are indicated with yellow arrowheads in an enlarged image of the left rectangle (top middle, scale bar: 100 μm). The axonal projections were observed in the CMM as shown in the enlarged image of the right rectangle (top right, scale bar: 200 μm). While some axons were observed in the area ventral to the HVC (bottom left, scale bar: 500 μm), no axons were observed running into the HVC, which is more clearly shown in the enlarged image of HVC (bottom right, scale bar: 200 μm).

(C) The average number of neurons that expressed EYFP in a section (mean and SEM over three sections) in the birds that underwent the experiments described in Figure 3 at 90 DPH and the birds that underwent the same experiment but with social isolation (left). Ratio of the area detected as positively stained with GFP antibody between HVC and HVC-shelf in the left and right hemisphere in each isolated bird (mean over three sections and SEM) (right).

forebrain area, the NCM, to the premotor area, the HVC. However, there were some technical limitations to this study. In the current methods, GOIs were expressed in TS-responsive (not -selective) neurons, which included cells that responded non-selectively to zebra finch song. Therefore, it cannot be concluded that projections into the HVC were from the neurons selectively responsive to TS. Expressing CaCasp3/dtA in TS-responsive neurons likewise would have killed non-selective neurons, including inhibitory neurons. Decreasing inhibitory activity in the NCM network would compromise the auditory responsiveness of TS-selective neurons.[7] The number of ablated neurons was uncountable.

We found that TS-responsive neurons project to five areas in juveniles: the LMAN, AIV, CMM, HVC-Shelf, and HVC. However, tracing axons from single neurons was not possible, even in whole-brain samples, so we cannot determine if different populations of neurons project to each area. Our experiments also do not allow us to know if one subset of neurons projected to both the HVC and HVC-shelf and then retracted their axons only from the HVC. Alternatively, different subsets of neurons may each project to the HVC and HVC-shelf separately, and only the subset that projected to the HVC (including their cell body) may then disappear in adults.

Similarly, ablation of the TS-responsive NCM neurons also could impair all of its projections, including to the CMM, AIV, and LMAN, which are all involved in song learning. Therefore, we cannot discount the role of these other regions in guiding song learning. Future work to investigate what kind of information is carried in the NCM-HVC projection and/or experiments manipulating the NCM-HVC projection specifically are needed to tell us how their pruning described here

contributes to song learning. Further studies can also reveal if the axons of TS-responsive neurons project from the NCM to their targets exist already before or only after memory formation.

STAR★METHODS

Detailed methods are provided in the online version of this paper and include the following:

- KEY RESOURCES TABLE
- RESOURCE AVAILABILITY
  - Lead contact
  - Materials availability
  - Data and code availability
- EXPERIMENTAL MODEL AND STUDY PARTICIPANT DETAILS
  - Birds
- METHOD DETAILS
  - Song recording and playbacks
  - Virus construct and productions
  - Virus injection and GOI expression procedures
  - Tissue clearing and immunohistochemistry
  - Light-sheet fluorescence microscope (LSFM)
  - Bird brain map construction, image registration and annotation
- QUANTIFICATION AND STATISTICAL ANALYSIS
  - Quantification of axonal projections
  - Cell counts
  - Song analysis
  - Statistics

SUPPLEMENTAL INFORMATION

Supplemental information can be found online at https://doi.org/10.1016/j.celrep.2024.114196.

ACKNOWLEDGMENTS

This work was supported by WPI-IRCN and a JSPS KAKENHI Grant-in-Aid for Scientific Research (B) (#18H02531) and Grant-in-Aid for Scientific Research on Innovative Areas, "Dynamic Regulation of Brain Function by Scrap & Build System" (#17H05754 and #19H04743), "Hyper-Adaptability" (#22H04767), and "Adaptive Circuit Census" (#22H05515) to Y.Y.-S. and "Information Physics of Living Matters" (#19H05794) to Y.O.; a Japan Agency for Medical Research and Development grant (AMED; JP21dm0207112) to H.H.; and the Japan Science and Technology Agency (JST; JPMJCR20E2 and JPMJMS2025-14 to Y.O., JPMJFR204D and JPMJMS2024 to H.H., and JPMJCR20E5 and JPMJMS2022-14 to M.K.). We thank Drs. T.K. Hensch and M.J. Coleman for critical reading of manuscript and constructive suggestions on the study, Dr. C. Yokoyama for critical reading of an earlier version of the manuscript, Mrs. L. Chunyu and Dr. K. Hossain for their assistance in making the 3D zebra finch brain atlas, and Mrs. A. Oba for maintenance of experimental animals.

AUTHOR CONTRIBUTIONS

Y.Y.-S., M.I.M.L., and M.K. designed the experiments; M.I.M.L., Y.Y.-S., M.K., Y.M., and J.A.K.-M. conducted experiments; M.K. established custom-made LSFM; H.H. and M.T. developed the cFos-TetON system; M.S.-V. and K.W. provided CaCasp3 and dtA plasmids; Y.M. constructed and developed the viral vectors; D.T., M.K., Y.M., and Y.O. developed the 3D zebra finch brain map and registration program and analyzed the 3D image data; M.I.M.L., Y.Y.-S., M.K., D.T., and J.A.K.-M. analyzed the data; and Y.Y.-S., M.I.M.L., Y.M., M.K., and D.T. wrote the paper.

DECLARATION OF INTERESTS

The authors declare no competing interests.

Received: April 18, 2023
Revised: January 15, 2024
Accepted: April 19, 2024
Published: May 7, 2024

REFERENCES

1. Hensch, T.K., and Bilimoria, P.M. (2012). Re-opening Windows: Manipulating Critical Periods for Brain Development. Cerebrum *11*.
2. Eales, L.A. (1985). Song learning in zebra finches: some effects of song model availability on what is learnt and when. Anim. Behav. *33*, 1293–1300.
3. Morrison, R.G., and Nottebohm, F. (1993). F. Role of a telencephalic nucleus in the delayed song learning of socially isolated zebra finches. J. Neurobiol. *24*, 1045–1064.
4. Price, P.H. (1979). Developmental determinants of structure in zebra finch song. J. Comp. Physiol. Psychol. *93*, 260–277.
5. Bolhuis, J.J., and Gahr, M. (2006). Neural mechanisms of birdsong memory. Nat. Rev. Neurosci. *7*, 347–357.
6. London, S.E., and Clayton, D.F. (2008). Functional identification of sensory mechanisms required for developmental song learning. Nat. Neurosci. *11*, 579–586. https://doi.org/10.1038/nn.2103.
7. Yanagihara, S., and Yazaki-Sugiyama, Y. (2016). Auditory experience-dependent cortical circuit shaping for memory formation in bird song learning. Nat. Commun. *7*, 11946. https://doi.org/10.1038/ncomms11946.
8. Katic, J., Morohashi, Y., and Yazaki-Sugiyama, Y. (2022). Neural circuit for social authentication in song learning. Nat. Commun. *13*, 4442. https://doi.org/10.1038/s41467-022-32207-1.
9. Vates, G.E., Broome, B.M., Mello, C.V., and Nottebohm, F. (1996). Auditory Pathways of Caudal Telencephalon and Their Relation to the Song System of Adult Male Zebra Finches (Taenopygia guttata). J. Comp. Neurol. *366*, 613–642.
10. Reijmers, L.G., Perkins, B.L., Matsuo, N., and Mayford, M. (2007). Localization of a stable neural correlate of associative memory. Science *317*, 1230–1233. https://doi.org/10.1126/science.1143839.
11. Liu, X., Ramirez, S., Pang, P.T., Puryear, C.B., Govindarajan, A., Deisseroth, K., and Tonegawa, S. (2012). Optogenetic stimulation of a hippocampal engram activates fear memory recall. Nature *484*, 381–385. https://doi.org/10.1038/nature11028.
12. Ye, L., Allen, W.E., Thompson, K.R., Tian, Q., Hsueh, B., Ramakrishnan, C., Wang, A.-C., Jennings, J.H., Adhikari, A., Halpern, C.H., et al. (2016). Wiring and Molecular Features of Prefrontal Ensembles Representing Distinct Experiences. Cell *165*, 1776–1788. https://doi.org/10.1016/j.cell.2016.05.010.
13. Sánchez-Valpuesta, M., Suzuki, Y., Shibata, Y., Toji, N., Ji, Y., Afrin, N., Asogwa, C.N., Kojima, I., Mizuguchi, D., Kojima, S., et al. (2019). Corticobasal ganglia projecting neurons are required for juvenile vocal learning but not for adult vocal plasticity in songbirds. Proc. Natl. Acad. Sci. USA *116*, 22833–22843. https://doi.org/10.1073/pnas.1913575116.
14. Price, P.H. (1979). Developmental determinants of structure in zebra finch song. J. Comp. Physiol. Psychol. *93*, 260–277. https://doi.org/10.1037/h0077553.
15. Williams, H., Kilander, K., and Sotanski, M.L. (1993). Untutored song, reproductive success and song learning. Anim. Behav. *45*, 695–705. https://doi.org/10.1006/anbe.1993.1084.
16. Fehér, O., Wang, H., Saar, S., Mitra, P.P., and Tchernichovski, O. (2009). De novo establishment of wild-type song culture in the zebra finch. Nature *459*, 564–568. https://doi.org/10.1038/nature07994.
17. Kelley, D.B., and Nottebohm, F. (1979). Projections of a telencephalic auditory nucleus -Field L-in the canary. J. Comp. Neurol. *183*, 455–469.

18. Fortune, E.S., and Margoliash, D. (1995). Parallel pathways and convergence onto HVc and adjacent neostriatum of adult zebra finches (Taeniopygia guttata). J. Comp. Neurol. *360*, 413–441. https://doi.org/10.1002/cne.903600305.

19. Shaevitz, S.S., and Theunissen, F.E. (2007). Functional connectivity between auditory areas field L and CLM and song system nucleus HVC in anesthetized zebra finches. J. Neurophysiol. *98*, 2747–2764.

20. Mandelblat-Cerf, Y., Las, L., Denisenko, N., and Fee, M.S. (2014). A role for descending auditory cortical projections in songbird vocal learning. Elife *3*, e02152. https://doi.org/10.7554/eLife.02152.

21. Canopoli, A., Herbst, J.A., and Hahnloser, R.H.R. (2014). A Higher Sensory Brain Region Is Involved in Reversing Reinforcement-Induced Vocal Changes in a Songbird. J. Neurosci. *34*, 7018–7026.

22. Tomaszycki, M.L., and Blaine, S.K. (2014). Temporary inactivation of NCM, an auditory region, increases social interaction and decreases song perception in female zebra finches. Behav. Proc. *108*, 65–70.

23. Doupe, A.J., and Konishi, M. (1991). Song-selective auditory circuits in the vocal control system of the zebra finch. Proc. Natl. Acad. Sci. USA *88*, 11339–11343. https://doi.org/10.1073/pnas.88.24.11339.

24. Solis, M.M., and Doupe, A.J. (1997). Anterior Forebrain Neurons Develop Selectivity by an Intermediate Stage of Birdsong Learning. J. Neurosci. *17*, 6447–6462. https://doi.org/10.1523/JNEUROSCI.17-16-06447.

25. Janata, P., and Margoliash, D. (1999). Gradual Emergence of Song Selectivity in Sensorimotor Structures of the Male Zebra Finch Song System. J. Neurosci. *19*, 5108–5118. https://doi.org/10.1523/JNEUROSCI.19-12-05108.

26. Sober, S.J., and Brainard, M.S. (2009). Adult birdsong is actively maintained by error correction. Nat. Neurosci. *12*, 927–931. https://doi.org/10.1038/nn.2336.

27. Warren, T.L., Tumer, E.C., Charlesworth, J.D., and Brainard, M.S. (2011). Mechanisms and time course of vocal learning and consolidation in the adult songbird. J. Neurophysiol. *106*, 1806–1821.

28. Innocenti, G.M., and Price, D.J. (2005). Exuberance in the development of cortical networks. Nat. Rev. Neurosci. *6*, 955–965. https://doi.org/10.1038/nrn1790.

29. Molnár, Z., Adams, R., and Blakemore, C. (1998). Mechanisms underlying the early establishment of thalamocortical connections in the rat. J. Neurosci. *18*, 5723–5745.

30. Herrmann, K., and Arnold, A.P. (1991). The development of afferent projections to the robust archistriatal nucleus in male zebra finches: a quantitative electron microscopic study. J. Neurosci. *11*, 2063–2074.

31. Bottjer, S.W. (2004). Developmental Regulation of Basal Ganglia Circuitry during the Sensitive Period for Vocal Learning in Songbirds. Ann. N. Y. Acad. Sci. *1016*, 395–415. https://doi.org/10.1196/annals.1298.037.

32. Kittelberger, J.M., and Mooney, R. (1999). Lesions of an avian forebrain nucleus that disrupt song development alter synaptic connectivity and transmission in the vocal pre-motor pathway. J. Neurosci. *19*, 9385–9398.

33. Schenk, A., Guido, P., and Heinz-Otto, P. (2000). Efficient Semiautomatic Segmentation of 3D Objects. Medical Images. International Conference on Medical Image Computing and Computer-Assisted Intervention (Springer), pp. 186–195.

34. Yagou, H., and Ohtake, Y. (2002). Belyaev G.A. Mesh smoothing via mean and median filtering applied to face normals. Geometric modeling and processing. Theory and applications. Gmp 2002. Proceedings. IEEE, 124–131.

35. Mattes, D., Haynor, D.R., Vesselle, H., Lewellyn, T.K., and Eubank, W. (2001). Nonrigid multimodality image registration. Medical Imaging 2001: Image Process. 4322. https://doi.org/10.1117/12.431046.

36. Vercauteren, T., Pennec, X., Perchant, A., and Ayache, N. (2008). Symmetric Log-Domain Diffeomorphic Registration: A Demons-Based Approach. International Conference on Medical Image Computing and Computer-Assisted Intervention (Springer), pp. 754–761.

37. Lorenzi, M., Ayache, N., Frisoni, G.B., and Pennec, X.; Alzheimer's Disease Neuroimaging Initiative ADNI (2013). LCC-Demons: a robust and accurate symmetric diffeomorphic registration algorithm. Neuroimage *81*, 470–483. https://doi.org/10.1016/j.neuroimage.2013.04.114.

38. Schindelin, J., Arganda-Carreras, I., Frise, E., Kaynig, V., Longair, M., Pietzsch, T., Preibisch, S., Rueden, C., Saalfeld, S., Schmid, B., et al. (2012). Fiji: an open-source platform for biological-image analysis. Nat. Methods *9*, 676–682. https://doi.org/10.1038/nmeth.2019.

STAR★METHODS

KEY RESOURCES TABLE

REAGENT or RESOURCE	SOURCE	IDENTIFIER
Antibodies		
anti-GFP	Molecular Probes	Cat# A-11122 RRID: AB_221569
Alexa Fluor 488 Goat anti-Rabbit IgG (H + L) Secondary Antibody	Thermo Fisher Scientific	Cat# A-11008 RRID: AB_143165
Alexa Fluor 405 Goat anti-Rabbit IgG (H + L) Secondary Antibody	Thermo Fisher Scientific	Cat# A-31556 RRID: AB_221605
Goat anti-Rabbit IgG (H + L), CF633 Conjugated	Biotium	Cat# 20122-1 RRID: AB_10853773
Bacterial and virus strains		
AAV2/9-cFos-TetON-EYFP-PEST	This study	N/A
AAV2/9-cFos-TetON-EGFP	This study	N/A
AAV2/9-cFos-TetON-CaCasp3	This study	N/A
AAV2/9-cFos-TetON-dtA	This study	N/A
Chemicals, peptides, and recombinant proteins		
DeepLabel A solution	Logos Biosystems	Cat# C33002
DeepLabel B solution	Logos Biosystems	Cat# C33003
X-CLARITY mounting solution	Logos Biosystems	Cat# C13101
DAPI (4′,6-Diamidin-2-phenylindole)	Dojindo	Cat# D523
Fluoromount	Diagnostic BioSystems	Cat# K024
PI (Propidium iodide)	Thermo Fisher Scientific	Cat# BMS500PI
NeuroTrace 640/660	Thermo Fisher Scientific	Cat# N-21483
Benzonase	Merck	Cat# E1014
Doxycycline hyclate	Merck	Cat# 324385-1GMCN
Silicone Oil	Shin-Etsu Chemical	Cat# KF-53, KF-50
Experimental models: Cell lines		
AAV-293 cell	Agilent	Cat# 240073 RRID: CVCL_6871
Experimental models: Organisms/strains		
Zebra finches (Taeniopygia guttata)	Yazaki-Sugiyama Lab (Univ of Tokyo and OIST)	
Recombinant DNA		
pAdDeltaF6	Addgene	RRID: Addgene_112867
pAAV2/9n	Addgene	RRID: Addgene_112865
pAAV-cFos-TetON-EYFP-PEST	This study	N/A
pAAV-cFos-TetON-EGFP	This study	N/A
pAAV-cFos-TetON-CaCasp3	This study	N/A
pAAV-cFos-TetON-dtA	This study	N/A
Software and algorithms		
Sound Analysis Pro 2011	Tchernichovski et al., 2000	http://soundanalysispro.com/
Avisoft-RECORDER	Avisoft Bioacoustics	RRID: SCR_014436
Avisoft-SASLabPro	Avisoft Bioacoustics	RRID: SCR_014438
GoldWave	Goldwave Inc.	https://www.goldwave.com/release.php
Fiji	ImageJ	RRID: SCR_002285
AIVIA	Leica Microsystems	https://www.aivia-software.com/

(*Continued on next page*)

Continued

REAGENT or RESOURCE	SOURCE	IDENTIFIER
MATLAB	MathWorks	www.mathworks.com
OriginPro2016	OriginLab	https://www.originlab.com/
Other		
Nanoject III	Drummond	Cat# 3-000-207
C417 PP lavalier microphone	AKG	Cat# 2577X00120
Nikon A1R confocal microscope	Nikon	RRID: SCR_020317
Leica TCS SP8 confocal microscope	Leica Microsystems	N/A (discontinued)
X-CLARITY Tissue Clearing System	Logos Biosystems	Cat# C30001
Fast Track Ultra 8R	M-AUDIO	N/A (discontinued)
Lightsheet Fluorescence Microscopy System	This study	N/A
(MVX10 Macroview Stereo Fluorescence Microscope) (PCO.edge Cooled sCMOS Camera) (OBIS LX/LS Lasers)	(Olympus/Evident) (PCO/Excelitas) (Coherent)	(RRID: SCR_018612) (www.excelitas.com) (www.coherent.com)

RESOURCE AVAILABILITY

Lead contact

Further information and requests for resources and reagents should be directed to and will be fulfilled by the lead contact, Yoko Yazaki-Sugiyama (yazaki-sugiyama@oist.jp).

Materials availability

Materials generated in this study will be available upon requests to the lead contact, Yoko Yazaki-Sugiyama (yazaki-sugiyama@oist.jp), but we may require a completed materials transfer agreement.

Data and code availability

The datasets generated during and/or analyzed during the current study are available from the lead contact, Yoko Yazaki-Sugiyama (yazaki-sugiyama@oist.jp) upon requests.

The computer codes we generated during the current study is available in the supplemental information.

Any additional information required to reanalyze the data reported in this work paper is available from the Lead Contact, contact, Yoko Yazaki-Sugiyama (yazaki-sugiyama@oist.jp) upon request.

EXPERIMENTAL MODEL AND STUDY PARTICIPANT DETAILS

Birds

Experiments were performed in accordance with experimental protocols approved by the animal care or biosafety committee at the medical school in The University of Tokyo or OIST Graduate University. Fifty-one male zebra finches, hatched and reared in our colony in the University of Tokyo, were used. As we focused on singing behaviors which are unique to males in this study, only males were used. The normally reared birds (N = 50) were raised in cages with their parents and siblings until at least ~60 DPH, or otherwise stated in the text for virus injection. Five birds (Isolated birds) were raised by their parents until 10–12 DPH when their father was removed from the cages, and then housed in the sound attenuation chamber with their siblings and a mother util they were subjected to an experiment. Additional 11 male zebra finches, hatched and reared in the colony of the OIST Graduate university were raised with their parents until they were injected with the virus and sacrificed at about 55–75 DPH.

METHOD DETAILS

Song recording and playbacks

Birds were periodically housed individually in a cage placed in a sound attenuation chamber and songs which were naturally emitted were recorded. The sounds produced inside a sound attenuation chamber were monitored and recorded using an Avisoft-RECORDER (Avisoft Bioacoustics, digitized at 32 kHz)) through a microphone (lavalier microphone, C417 PP, AKG) connected to an audio interface (Fast Track Ultra 8R, M-AUDIO). Sounds which exceeded a user-defined threshold were automatically saved as wave files.

Recorded songs were also used for song stimulation. The recorded songs were high pass filtered at 400 Hz and normalized the volume, then trimmed by eliminating non-song vocalizations then used as a song stimulation by combining multiple renditions with silent intervals for making it ~1 hr length.

Virus construct and productions

The AAV vectors of serotype 9 were generated by tripartite transfection (11 μg of pAAV2/9n plasmid (Addgene, #112865) which expresses Rep protein from serotype 2 and Cap protein from serotype 9, 20 μg of pAdDeltaF6 'Helper' plasmid (Addgene, #112867), and 10 μg of pAAV-vector plasmid encoding the gene of interest) into AAV-293 cells (Agilent, Santa Clara, CA, USA) cultured in 100 mm dishes using a standard calcium phosphate method. Three days after transfection, cells were collected, resuspended in PBS containing 5% sorbitol and 350 mM NaCl, and lysed by four rounds of freeze and thaw cycle. The nucleic acid component of the virus producer cells was removed by nuclease (Benzonase; Merck KGaA, Darmstadt, Germany) treatment followed by repeated clearing of cell debris. The resulting cleared lysates containing AAV particles (titer ranged 2.6–4.6 × 10^{12} vg/mL) were used for viral infections without concentration.

Virus injection and GOI expression procedures

For expressing EYFP in the neurons which were activated under the doxycycline (DOX, Merck KGaA, Darmstadt, Germany) condition, AAVs (AAV2/9-cFos-TetON-EYFP-PEST, the birds which were tested at 70, 80 and 90 DPH (Figure 6) were injected with AAV2/9-cFos-TetON-EGFP) (total, 200–300 nL/hemisphere) were injected through a glass pipet connected to a pressure injector (Nanoject III; Drummond Scientific Company, Broomall, PA, USA) to the zebra finch brain targeting to the NCM with stereotaxic coordination (0.5 mm lateral, 0.5 mm anterior from the Y sinus, 2.1 mm depth) under isoflurane anesthesia (2-3 %). After the virus injection, birds were individually isolated in a sound attenuation chamber for 12–20 days, and were provided with DOX in the drinking water (0.4 mg/mL) and song stimulation for two days (song: 1 h/day). Then the virus injected birds were transcardially perfused under deep anesthesia with pentobarbital at five days after the first day of DOX applications for histological analysis.

For control experiments, adult birds (>120 DPH) were injected with AAVs (AAV2/9-cFos-TetON-EYFP-PEST) and individually isolated as described above. Nine birds were provided with DOX in the drinking water (0.4 mg/mL) with TS playbacks for two days as described above and sacrificed one, three or seven days after the first day of DOX applications for histological analysis (Figure S2A). Although not significant, there was a small number of EYFP expressing neurons in NCM when birds were sacrificed three days after DOX administration. To expect maximum EYFP expression, we sacrificed birds five days after DOX. Three birds were provided with DOX in the drinking water (0.4 mg/mL) with no song stimulation for two days, then were perfused at five days after the first day of DOX applications for histological analysis (no song control) (Figures S2B and S2C). Another three birds were exposed to a novel zebra finch song playback (CON: conspecific songs) together with DOX administration instead of TS playback and processed for histological analysis as described above (CON control).

For ablating tutor song responding neurons in the NCM, a mixture of the virus vectors (AAV2/9-cFos-TetON-CaCasp3 and AAV2/9-cFos-TetON-dtA, 1:1) was injected (total, 200–300 nL/hemisphere) into NCM as described above at ~40 DPH (35–42 DPH), or ~70 DPH (66–70 DPH). After the virus injection the birds were again housed together with their parents until they were provided with DOX in water (0.4 mg/mL) and 1-h long tutors' song playback for two days starting at ~50 DPH (48–52 DPH) or ~90 DPH (84–91 DPH). The birds were isolated in a sound attenuation chamber until at least 120 DPH at which point they were sacrificed. The control siblings were provided with DOX water and no song playbacks. The birds, which were injected with the virus at ~40 DPH, were exposed to the second tutor at ~70 DPH together with control siblings. Their songs were occasionally recorded.

Tissue clearing and immunohistochemistry

For making cleared brain samples, brains were post-fixed with 4% PFA for overnight at 4°C and washed with PBS for one day, then incubated with polymerization solutions (A4P0) for three to five days at 4°C. Then the samples were polymerized at 37°C in a vacuumed chamber for several hours. After being washed with PBS for a day, the brain tissues were then subjected to electrophoresis for several hours with an X-CLARITY Tissue clearing system (Logos Biosystems, South Korea). Then the cleared brain samples were subject to immunohistochemical staining process with a DeepLabel antibody staining kit (Logos Biosystems). After the electrophoresis solution was washed out with PBS for a day, brain samples were incubated with DeepLabel A solution (Logos Biosystems, Cat# C33002) overnight, then with pre-incubated antibody mixture and PI (propidium iodide, Thermo Fisher Scientific, Cat# BMS500PI) for counter staining in the DeepLabel B solution (Logos Biosystems, Cat# C33003) at room temperature for 10–14 days. Primary and secondary antibodies were pre-incubated in a small amount in DeepLabel B solution (50 μL) at 37°C for 90 min in advance (1:100 anti-GFP (Molecular Probes, Cat# A-11122) and 1:150 Alexa Fluor 488 conjugated anti rabbit IgG secondary antibody (Thermo Fisher Scientific, Cat# A-11008)). After washing out the antibody solution with PBS for a day, brain samples were incubated with X-CLARITY mounting solution (Logos Biosystems, Cat# C13101) and embedded in agar for imaging with the custom-made light-sheet fluorescence microscope.

All the brain sections from the birds which were injected with AAV2/9-cFos-TetON-EYFP-PEST were stained immunohistochemically to enhance EYFP signals. For immunohistochemical staining in conventional sections, brain tissues were post-fixed and cryoprotected overnight in 15% sucrose in 4% PFA solution. The brains were cut sagittally first, and forty-μm thickness sections were taken from the medial edge of the brain to the lateral edge of HVC (60–70 sections/hemisphere), were made and incubated

with primary anti-GFP antibody (Molecular Probes, Cat# A-11122) for 48 h at 4°C (1:1000 in 0.3% Triton X-100/PBS). After washing primary antibody with PBS, the sections were incubated with secondary antibody (Alexa Fluor 405 goat anti-rabbit antibody, Thermo Fisher Scientific, Cat# A-31556) and NeuroTrace 640/660 (Thermo Fisher Scientific, Cat# N-21483) (1:300 for both in PBS) overnight at 4°C. Sections were then mounted on slide glasses and cover-slipped with mounting medium (Fluoromount, Diagnostic BioSystems, Cat# K024). Confocal images of three sections including HV, HVC-Shelf and injected NCM brain area were taken from each bird using the confocal microscope (Nikon A1R) with a 20x objective. Images were analyzed for axonal projection or cell counts as described below. For the birds used in Figure 6 ($N = 10$), fifty-μm thickness sections were made, incubated with primary anti-GFP antibody in 2% Triton X-100/PBS, secondary antibody (Goat anti-rabbit IgG antibody, CF633 conjugated, Biotium, Cat# 20122-1) and DAPI (4′,6-Diamidin-2-phenylindole, 1:2000, Dojindo, Cat# D523). Images were taken with confocal microscope (Leica TCS SP8) with a 20x objective.

Light-sheet fluorescence microscope (LSFM)

We developed a novel LSFM system with spatially uniform thin light-sheet illumination which provided a three-dimensionally isotropic resolution and covered an entire area of brain samples at each z-position. Light-sheet illumination was horizontally generated by scanning a focused Gaussian beam, and the emitted fluorescence signal was captured via macro-zoom microscope (MVX-10 and MVPLAPO0.63X, Olympus) and a cooled CMOS camera (pco.edge 5.5, PCO GmbH). The numerical aperture of the illumination beam was set to 0.05. The focal point of the beam was axially swept in the field of view (FOV) synchronous to the motion of the rolling shutter of the camera. The cleared and embedded brain sample was placed on the stage in a chamber filled with silicone oil (mixture of KF-53 and KF-50, Shin-Etsu Chemical). The refractive index of the sample and of the oil was tuned to 1.462 ± 0.002. Brain samples were excited by 488 nm and 532 nm laser sources (OBIS LS, Coherent) separately for imaging sparsely labeled neurons and their axons signal and cell nuclei signal stained with PI, respectively. The parasagittal images of each brain hemisphere were captured from lateral to medial by changing the vertical position of the chamber, z-step of which was set to equally to the x-y pixel size of each frame, which yielded 1500–2200 sections for each hemisphere at total magnitude 1.6–2.5 X.

Bird brain map construction, image registration and annotation

The 3D bird brain map for cleared whole brain samples were constructed for the major song related brain areas. The outlines of major zebra finch brain regions of every ten PI staining images were manually drawn with visual inspection first (reference brain), then were interpolated over for a hemisphere by using the shape-based interpolation technique[33] and triangulated and smoothed using a mean face normal filter.[34] To relate images of a given brain sample to corresponding brain regions in the reference brain, we performed a two-step image registration. First, PI staining images of a given sample were roughly registered to the reference brain images by an affine transformation with the mutual information as the similarity measure.[35] Next, the first rough registration was further refined by a nonlinear transformation, to which a log-domain diffeomorphic framework[36,37] was adopted. Transformations were gradually refined in a coarse-to-fine manner by starting the registration at 1/8 sampling ratio and recurring sequential up-sampling and registration by a factor 2. Then the inverse transformation of the registration was applied to the brain regions in the reference brain that resulted in annotating those brain regions in images of a given sample brain. During the procedure, obviously inaccurate registration and annotation results were corrected manually.

QUANTIFICATION AND STATISTICAL ANALYSIS

Quantification of axonal projections

To quantify axonal projections within HVC, outlines of HVC were drawn with NeuroTrace staining images by using the 'polygon selection' tool in FIJI.[38] The area of HVC-Shelf was defined as the same shape and size area just beneath (ventral to) the HVC. Anti-GFP positive areas were defined by unbiased image binarization, using the pixel classifier function in the computer software, AIVIA (Leica Microsystems, Inc.). The classifier was applied to the whole dataset, and was trained to detect anti-GFP positive pixels with the image training set comprising representative images from each hemisphere of all birds anti-GFP positive area within the HVC and HVC-Shelf were then measured with thresholding by using FIJI using a constant mean gray value. Mean gray value was set to include all pixels classified as anti-GFP positive by AIVIA pixel classifier. The anti-GFP positive area within the HVC and HVC-Shelf were measured for three representative sections from each hemisphere, then the ratio of anti-GFP positive area within the HVC vs. HVC-Shelf. Then the mean and SEM within each hemisphere and within a bird (average between both hemispheres) were calculated. Statistical comparisons for axon density indicated by a ratio of anti-GFP positive area between HVC and HVC-shelf between groups of birds were done by ANOVA with post hoc Tuckey LSD test.

Cell counts

For GFP positive cell counts, we used the image of native GFP expression, and the number of the GFP positive neurons was manually counted within NCM using the Cell Count Add-on functions in FIJI. The boarders of NCM, was determined as caudal to Field L to the rostral edge of the section and from dorsal to ventral edges. The cell number in three representative sections including NCM was counted in each hemisphere and the mean and SEM were calculated.

Song analysis

The songs were analyzed for song similarity by using Sound Analysis Pro software (SAP 2011). For each bird, 5 typical motives were randomly chosen and calculated song similarities between two songs by averaging the song similarity scores of all the possible combinations. Motif size of each song was calculated as an average of 10 randomly chosen song motives. Statistical comparison between experimental and control groups was done by One-way repeated measure ANOVA with post hoc Fisher's LSD test, and between experimental and control sibling was done by paired t-tests.

Statistics

Mean ± SEM was provided where specified (N represents the number of birds). Individual data were also plotted where applicable. Details about statistical analysis are given in the above respective sections. Description of statistics can be found in figure legends and the Results. All statistical tests were carried out using statical tools in the computer software, OriginPro2016 (OriginLab).